

# Parity-Time Symmetry in a Flat Band System

Li Ge<sup>1,2,\*</sup>

<sup>1</sup>Department of Engineering Science and Physics, College of Staten Island, CUNY, Staten Island, NY 10314, USA

<sup>2</sup>The Graduate Center, CUNY, New York, NY 10016, USA

(Dated: July 21, 2022)

In this report we introduce Parity-Time ( $\mathcal{PT}$ ) symmetric perturbation to a one-dimensional Lieb lattice, which is otherwise  $\mathcal{P}$ -symmetric and has a flat band. In the flat band there are a multitude of degenerate dark states, and the degeneracy  $N$  increases with the system size. The half-gain-half-loss perturbation we consider overlaps with the dark states, and we show that both randomly positioned states and pinned states at the symmetry plane in the flat band can undergo thresholdless  $\mathcal{PT}$  breaking. They are distinguished by their different rates of acquiring non-Hermiticity as the  $\mathcal{PT}$ -symmetric perturbation grows, which are insensitive to the system size. Using a degenerate perturbation theory, we derive analytically the rate for the pinned states, whose spatial profiles are also insensitive to the system size. Finally, we find that the presence of weak disorder has a strong effect on modes in the dispersive bands but not on those in the flat band. The latter response in completely different ways to the growing  $\mathcal{PT}$ -symmetric perturbation, depending on whether they are randomly positioned or pinned.

## I. INTRODUCTION

Systems that exhibit flat bands have attracted considerable interest in the past few years, including optical [1, 2] and photonic lattices [3–5], graphene [6, 7], superconductors [8–11], fractional quantum Hall systems [12–14] and exciton-polariton condensates [15, 16]. One interesting consequence of a flat band is the different scaling properties of its localization length when compared with a dispersive band [17–19], due to a multitude of degenerate states in the flat band. This degeneracy has another important implication on Parity-Time ( $\mathcal{PT}$ ) symmetry breaking [20–38]: it was found recently that the degeneracy of the underlying Hermitian spectrum, before any  $\mathcal{T}$ -breaking perturbations are introduced, determines whether thresholdless  $\mathcal{PT}$  symmetry breaking is possible [39].

Using a quasi-one-dimensional (quasi-1D) Lieb lattice (see Fig. 1) and a half-gain-half-loss perturbation overlapping with its degenerate states, we show in this report that two different scenarios of thresholdless  $\mathcal{PT}$  symmetry breaking can take place, depending on whether the degeneracy  $N$  in the flat band is even or odd. When  $N$  is odd, all but one flat band modes enter the  $\mathcal{PT}$ -broken phase at infinitesimal strength of  $\mathcal{T}$ -breaking perturbation. They form two  $(N - 1)/2$  degenerate branches, each confined strictly to either the gain half or the loss half of the lattice, and their non-Hermiticity equals that of the  $\mathcal{T}$ -breaking perturbation, which we denote by  $\tau$ . When  $N$  is even, all flat band modes experience thresholdless  $\mathcal{PT}$  breaking, but now they exhibit four branches. Two of them are  $(N/2 - 1)$  degenerate and have the same properties as those in the  $N$ -odd case. The remaining two form a  $\mathcal{PT}$ -symmetric doublet, and they are pinned at the symmetry plane  $x = 0$ , with exponential tails in both the

gain and the loss halves. Surprisingly, we find that this localization is not due to the half-gain-half-loss nature of the  $\mathcal{PT}$ -symmetric perturbation as previously found [40], but rather a result of its point defect at  $x = 0$  to satisfy the  $\mathcal{PT}$  symmetry. Therefore, this spatial profile is insensitive to both  $\tau$  and the system size when  $N$  is large, and it can be reproduced in the underlying Hermitian system at  $\tau = 0$ . Using a degenerate perturbation theory, we derive this localization length and the rate these doublet states acquire non-Hermiticity. Finally, we show that the presence of weak disorder has a strong

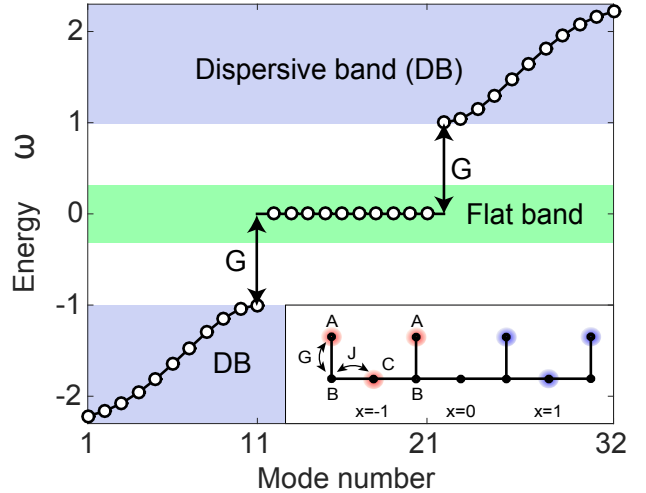


FIG. 1. (Color online) Inset: A quasi-1D Lieb lattice with 3 overlapping “ $A-B-C-B-A$ ” sublattices. Two dark states are shown schematically by circular clouds, which double as an example of a half-gain-half-loss  $\mathcal{PT}$  symmetric perturbation. Main figure: Energy of the eigenmodes in a Lieb lattice with 10-fold degeneracy in the flat band, calculated with  $\omega_A = \omega_B = \omega_C = 0$  and  $G = J = 1$ . There is one more mode in each of the two dispersive bands.

\* li.ge@csi.cuny.edu

effect on modes in the dispersive bands but not on those in the flat band. The finite  $\mathcal{PT}$ -transition thresholds of the former are smoothed out, while the thresholdless  $\mathcal{PT}$  breaking of the latter is largely preserved. In addition, the flat band modes response in completely different ways to increasing  $\mathcal{T}$ -breaking perturbation when there is disorder. The  $\mathcal{T}$ -breaking perturbation has little effect on them if they are already localized to either half of the lattice. Otherwise the perturbation forces them to pick a side, unless they are the doublet states, which evolve from Anderson localized states [41] to those pinned by the point defect at  $x = 0$ . We note that different from Refs. [26, 42], the system we consider here has a flat band *before* the  $\mathcal{T}$ -breaking perturbation is introduced, instead of being the result of  $\mathcal{PT}$ -symmetry breaking.

## II. THRESHOLDLESS $\mathcal{PT}$ BREAKING IN A LIEB LATTICE

In two-dimensional systems of a finite size, the maximum degeneracy due to a point group is 2. In a flat band, however, the degeneracy can be arbitrarily large, because it increases with the system size. Take a quasi-1D Lieb lattice for example (see Fig. 1), where an upright  $A$  site is decorated to every other site of a 1D chain (i.e., the  $B$  sites). A flat band exists when the onsite energy of  $A$  and  $C$  sites are the same,  $\omega_A = \omega_C \equiv \omega_0$  (see Fig. 1;  $\hbar = 1$ ), and  $\omega_0$  gives the flat band energy. It is gapped from the two dispersive bands by  $G$ , the real-valued coupling between two neighboring  $A$  and  $B$  sites. For simplicity we take  $\omega_B = \omega_0$  as well. Because  $\omega_0$  shifts all eigenvalues by the same amount and has no effect on the eigenstates, we take it to be zero. The degeneracy  $N$  of the flat band in this Lieb lattice equals the number of existing dark states, which we will denote by  $\vec{V}(x)$  due to their geometry (see the inset in Fig. 1). Each dark state has a nonvanishing amplitude only at a  $C$  site and two nearest  $A$  sites:

$$\vec{V}(x) = [J, 0, -G, 0, J]^T, \quad (1)$$

where the five elements are the amplitudes of the wave function on a “ $A$ – $B$ – $C$ – $B$ – $A$ ” sublattice, to which we will refer as  $U$  sublattices below. The  $B$  sites are black in  $\vec{V}(x)$  because the tunneling probabilities from the neighboring  $A$  and  $C$  sites cancel each other. The argument  $x$  in  $\vec{V}(x)$  is the position of the central  $C$  site of an  $U$  sublattice in the units of the lattice constant. It takes integer or half integer values, depending on whether  $N$  is odd or even, and the center of the lattice is placed at  $x = 0$ . We note that the number of (overlapping)  $U$  sublattices equals the number of dark states, and each end of the lattice is terminated on  $A$  and  $B$  sites. The superscript “ $T$ ” in Eq. (1) denotes matrix transpose, and  $J$  is the real-valued coupling between two neighboring  $B$  and  $C$  sites. Below we drop the vector symbol of  $\vec{V}(x)$  for simplicity.

The tight-binding Hamiltonian of the Lieb lattice can

be written as

$$\mathbf{H}_0 = \sum_{i,Z} \omega_Z |Z_i\rangle \langle Z_i| + \sum_i [G|A_i\rangle \langle B_i| + h.c.] + \sum_i [J(|B_i\rangle \langle C_i| + |C_i\rangle \langle B_{i+1}|) + h.c.], \quad (2)$$

where  $i$  runs through all unit cells,  $Z = A, B, C$ , and  $h.c.$  denotes Hermitian conjugate of the other terms in the brackets. We then introduce the  $\mathcal{T}$ -breaking perturbation  $i\tau\mathbf{H}_1$ , which is  $\mathcal{PT}$ -symmetric about  $x = 0$ .  $\tau$  is the overall strength of the  $\mathcal{T}$ -breaking perturbation, and  $\mathbf{H}_1$  is a diagonal matrix with positive (loss) or negative (gain) elements.

One may expect that the construction of the flat band states in the  $\mathcal{PT}$ -broken phase should be straightforward: all one needs are two dark states symmetrically placed about  $x = 0$  and linearly superposed as

$$f_1(x) = V(x) + iaV(-x), \quad (3)$$

$$f_2(x) = V(-x) - iaV(x), \quad (4)$$

where  $a$  is a real parameter that may depend on  $\tau$ .  $f_1, f_2$  can be easily shown to be  $\mathcal{PT}$ -symmetric partners, i.e.,  $f_1(x) = \mathcal{PT}f_2(x)$ , by considering that the dark states have a real-valued wave function (see Eq. (1)). This conjecture is one possible construction only when  $V(x), V(-x)$  do not overlap with  $x = 0$  and when each of the two corresponding  $U$  sublattices has the same gain or loss on  $A$  and  $C$  sites, which we will refer to as the “ $V$ ” configuration. The corresponding  $\mathbf{H}_1$  has diagonal elements  $0, \pm 1$ , which are anti-symmetric about  $x = 0$  to satisfy the  $\mathcal{PT}$  symmetry (see the inset of Fig. 1, for example). In this case we find  $a = 0$ , i.e., two isolated dark states  $V(-x)$  and  $V(x)$  are  $\mathcal{PT}$  symmetric partners of each other. This is because  $V(-x), V(x)$  are eigenstates of both  $\mathbf{H}_0$  and  $\mathbf{H}_1$  in the “ $V$ ” configuration, but with opposite real eigenvalues for  $\mathbf{H}_1$ . As a result, the imaginary parts of the corresponding eigenvalues are nothing but  $\kappa_{\pm} \equiv \text{Im}[\tilde{\omega}_{\pm}] = \pm\tau$  (see Fig. 2), which are independent of the system size and the couplings  $G, J$ . In other words, these dark states enter the  $\mathcal{PT}$ -broken phase at infinitesimal value of  $\tau$  [39], and their non-Hermiticity (given by  $|\kappa_{\pm}|$ ) is the same as the  $\mathcal{T}$ -breaking perturbation (i.e.,  $\tau$ ).

Note that two overlapping  $U$  sublattices share one  $A$  and one  $B$  site. Therefore, the “ $V$ ” configuration of  $\mathbf{H}_1$ , when spatially extended to more than one pair of symmetrically placed  $U$  sublattices, requires the same gain or loss on all the  $A$  and  $C$  sites of these  $U$  sublattices, with the longest one being a half-gain-half-loss configuration. In such extended “ $V$ ” configurations, there can be more than one pair of dark states that undergo thresholdless  $\mathcal{PT}$  breaking simultaneously. More specifically, when all  $A$  and  $C$  sites on the positive (negative)  $x$ -axis have the same gain and their counterparts on the negative (positive)  $x$ -axis have the same loss, there are  $(N - 1)/2$  such pairs of dark states when  $N$  is odd (e.g., 2 and 3 pairs for the  $N = 5, 7$  cases shown in Figs. 2(a) and 4(a)) and  $(N/2 - 1)$  such pairs when  $N$  is even (e.g., 2 and 3

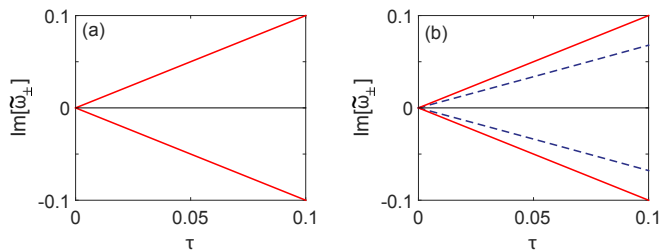


FIG. 2. (Color online) Thresholdless  $\mathcal{PT}$  breaking in a Lieb lattice with half-gain-half-loss “V” configuration. (a)  $N = 5$ . 4 flat band modes enter the  $\mathcal{PT}$ -broken phase at  $\tau = 0$  (thick solid lines). The other flat band mode and all 12 dispersive band modes remain in the symmetric phase in the range of  $\tau$  shown (thin solid line). (b)  $N = 6$ . All 6 flat band modes enter the  $\mathcal{PT}$ -broken phase at  $\tau = 0$ , 4 with  $\kappa_{\pm} = \pm\tau$  (thick solid lines) and 2 with  $|\kappa_{\pm}| < \tau$  (dashed lines). All 14 dispersive band modes remain in the symmetric phase in the range of  $\tau$  shown (thin solid line).

pairs for the  $N = 6, 8$  cases shown in Fig. 2(b) and 4(b)), which are the numbers of  $U$  sublattices that do not have a site at  $x = 0$  in these two cases. This observation also indicates that each of the two  $\kappa_{\pm} = \pm\tau$  branches has  $(N - 1)/2$  ( $N$ -odd) or  $N/2 - 1$  ( $N$  even) degeneracy in the  $\mathcal{PT}$ -broken phase. Such a large number of degenerate states in the  $\mathcal{PT}$ -broken phase has not been reported before.

For the single dark state  $V(x = 0)$  that is left alone in the  $N$ -odd case, it is no longer an eigenstate of  $\mathbf{H}_1$  since there is no  $\mathcal{T}$ -breaking perturbation on the  $C$  site at  $x = 0$  to respect the  $\mathcal{PT}$  symmetry. Hence it needs to couple to modes in the dispersive bands to break the  $\mathcal{PT}$  symmetry, which then leads to a finite threshold in terms of  $\tau$ . The two dark states  $V(x = -1/2)$  and  $V(x = 1/2)$  in the  $N$ -even case are not eigenstates of  $\mathbf{H}_1$  either, due to the absence of  $\mathcal{T}$ -breaking perturbation on the  $A$  site at  $x = 0$  to respect the  $\mathcal{PT}$  symmetry. We will refer to these two states as the doublet states. Although they do not belong to the  $(N/2 - 1)$  degenerate manifolds of the two  $\kappa_{\pm} = \pm\tau$  branches, they still experience a thresholdless  $\mathcal{PT}$  breaking, but their  $|\kappa_{\pm}|$  is smaller than  $\tau$  (see Fig. 2(b)). Interestingly, we find that the slope of these  $|\kappa_{\pm}|$  is also insensitive to the system size  $N$ , when  $N > 2$ . More specifically, this slope is about 0.708, 0.675, 0.671, 0.670 when  $N = 2, 4, 6, 8$ , measured by  $\kappa'_+(\tau = 0.1) \approx \left. \frac{\kappa_+(\tau)}{\tau} \right|_{\tau=0.1}$  (see Fig. 2(b)).

To understand this property, we resort to two approaches, a qualitative one based on directly visualizing the spatial profiles of the doublet states, and a quantitative one based on a degenerate perturbation theory. As Fig. 3(a) shows, the doublet states are pinned near  $x = 0$  and have tails in both the gain and the loss halves of the lattice. We find that these spatial profiles are also insensitive to the system size when  $N$  is large enough ( $> 2$ ; see Figs. 3(a) and (b)), which explains the same

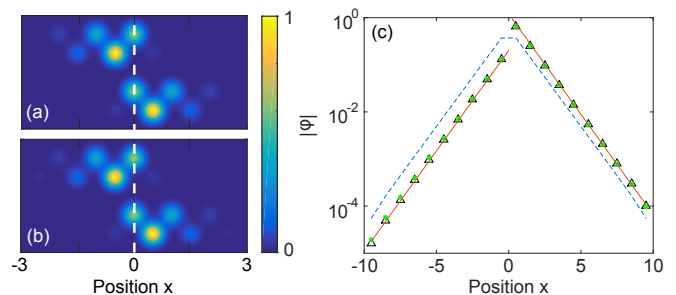


FIG. 3. (Color online) Doublet states in the  $\mathcal{PT}$ -broken phase with half-gain-half-loss “V” configuration. (a) False color plot of the absolute value of their wave functions for  $N = 6$ . The vertical dashed line marks  $x = 0$ . (b) Same as (a) but for  $N = 20$ . (c) Exponential tails of the amplifying doublet state shown in (b). Only the absolute value of the wave function on the  $C$  sites is shown. Filled dots and open squares are calculated at  $\tau = 0.002$  and  $0.2$ , respectively. Solid lines are proportional to  $\exp(-|x|/1.03)$  shown for comparison. Dashed line shows the defect state at  $\tau = 0$  by increasing  $\omega_A(x = 0)$  to  $0.1$ .

property of their  $\kappa_{\pm}$ . In fact, we find the tails of their spatial profiles decay exponentially away from  $x = 0$  (see Fig. 3(c)). One might expect that these exponential tails are a result of gain and loss, as it has been shown that the wave function in the  $\mathcal{PT}$ -broken phase tends to peak at the gain and loss interface [40]. However, we find the exponential tails are largely independent of the  $\mathcal{T}$ -breaking perturbation strength, either. As Fig. 3(c) shows, the tails are captured well by an exponent of  $-|x|/1.03$ , and there is little change in the wave function when  $\tau$  changes from  $0.002$  to  $0.2$ . Instead, we find that this localization length of  $\xi = 1.03$  is due to the point defect of the “V” configuration at  $x = 0$ , which has neither gain or loss on the  $A$  site at  $x = 0$  to respect the  $\mathcal{PT}$  symmetry as mentioned. If we introduce a point defect at  $x = 0$  in the Hermitian system at  $\tau = 0$ , for example, by increasing  $\omega_a$  here to  $0.1$ , we recover the same localization length (see the dashed line in Fig. 3(c)).

Before we derive the perturbation theory for the doublet states, we briefly discuss the modes in the dispersive bands. They have very high  $\mathcal{PT}$ -transition thresholds when  $N$  is small. This observation can be understood in the following way: their eigenvalues are distributed in  $|\omega| \in [\omega_0 + G, \omega_0 + \sqrt{G^2 + 4J^2}]$  (see Fig. 1) and are well separated from each other when  $N$  is small; their thresholds are proportional to these spacings, in the simplest case of two-mode coupling [39]. As  $N$  increases, their energy spacings reduce and so do their  $\mathcal{PT}$ -transition thresholds. For example, no dispersive band modes enter the  $\mathcal{PT}$ -broken phase in Fig. 2, but their lowest threshold reduces to  $\tau \approx 0.090$  and  $0.072$  for  $N = 7$  and  $8$ , respectively (see Fig. 4). Due to the symmetry of the dispersive bands about  $\omega_0 = 0$  (see Fig. 1), when one pair of dispersive band modes enter the  $\mathcal{PT}$ -broken phase at some finite value of  $\tau$ , there is always another pair do the same at exactly the same  $\tau$

but at the opposite energy; their  $\kappa_{\pm}$  are nevertheless the same.

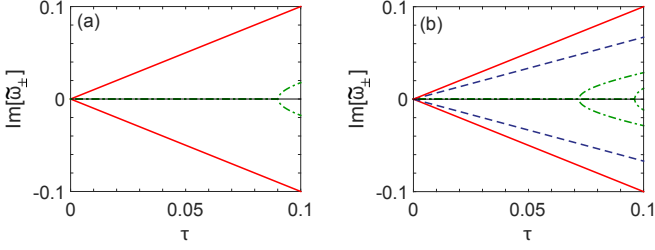


FIG. 4. (Color online) Same as Fig. 2 but with  $N = 7$  in (a) and  $N = 8$  in (b). 4 and 8 dispersive band modes in (a) and (b) enter the  $\mathcal{PT}$ -broken phase before  $\tau = 0.1$ , respectively (dash-dotted lines). Note the features of the flat band modes (solid and dashed lines) are the same as in Fig. 2. Horizontal thin lines represent modes in the  $\mathcal{PT}$  symmetric phase.

### III. DEGENERATE PERTURBATION THEORY

Now we turn to the perturbation theory for a more quantitative understanding of the doublet states, and hence  $N$  considered in this section is even. We start by diagonalizing the perturbation  $\mathbf{H}_1$  in the  $N$ -fold flat band subspace of  $\mathbf{H}_0$ , which is required in the degenerate perturbation theory [43]. In the  $N = 2$  case, we define the basis in this subspace as  $\phi_1^{(2)} = V(-1/2) + aV(1/2)$  and  $\phi_2^{(2)} = bV(-1/2) + V(1/2)$ , where we can take  $a, b$  to be real numbers, because  $\mathbf{H}_1$  (without the factor  $i\tau$ ) is Hermitian. The superscript enclosed in parentheses indicates the value of  $N$ . The above requirement then means  $\langle \phi_1^{(2)} | \mathbf{H}_1 | \phi_2^{(2)} \rangle = 0$ , and an additional constraint is  $\langle \phi_1^{(2)} | \phi_2^{(2)} \rangle = 0$ . We note that this requirement is different from demanding that  $\phi_1^{(2)}, \phi_2^{(2)}$  are the eigenstates of  $\mathbf{H}_1$ ; the latter is sufficient but unnecessary, as it implies that  $\mathbf{H}_1$  is diagonal in the whole Hilbert space of the eigenstates of  $\mathbf{H}_0$ , not just its  $N$ -fold flat band subspace.

Since the flat band states are dark on  $B$  sites, we can project the wave functions and  $\mathbf{H}_1$  to the Hilbert space of  $A$  and  $C$  sites, leading to  $V(-1/2) = [J, -G, J, 0, 0]^T$ ,  $V(1/2) = [0, 0, J, -G, J]^T$ , and  $\mathbf{H}_1 = \text{diag}(1, 1, 0, -1, -1)$  when  $N = 2$ , where “diag” stands for a diagonal matrix. Using  $\langle \phi_1^{(2)} | \mathbf{H}_1 | \phi_2^{(2)} \rangle = 0$  we find  $a = b$ , and  $\langle \phi_1^{(2)} | \phi_2^{(2)} \rangle = 0$  leads to

$$a = \pm \sqrt{\left(2 + \frac{G^2}{J^2}\right)^2 - 1} - \left(2 + \frac{G^2}{J^2}\right). \quad (5)$$

Note that the two values of  $a$  are reciprocal of each other, which means that if one leads to  $\phi_1^{(2)}$ , the other one gives  $\phi_2^{(2)}$ . By neglecting the coupling to the dispersive band

modes, we then derive

$$|\kappa_{\pm}^{(2)}(\tau)| = \left| \frac{\langle \phi_1^{(2)} | \mathbf{H}_1 | \phi_1^{(2)} \rangle}{\langle \phi_1^{(2)} | \phi_1^{(2)} \rangle} \right| \tau = \left| \frac{a^2 - 1}{2a} \right| \frac{J^2}{3J^2 + G^2} \tau \quad (6)$$

for the doublet states, which gives a slope of 0.707 when  $G = J = 1$ . Using  $\phi_2^{(2)}$  in the expression above leads to the same result. Previously we have mentioned that the numerically obtained slope in this case is 0.708, calculated using  $\kappa'_{\pm}(\tau = 0.1) \approx \frac{\kappa_{\pm}(\tau)}{\tau} \Big|_{\tau=0.1}$ . If we reduce the perturbation strength at which the slope is calculate, for example, to  $\tau = 0.02$ , we find  $\frac{\kappa_{\pm}(\tau)}{\tau} \Big|_{\tau=0.02} = 0.707$ , which agrees nicely with the analytical result given by Eq. (6). Since the slope of  $|\kappa_{\pm}|$  given by Eq. (6) is independent of  $\tau$ , we know that any change to the slope has to be a result of coupling to the dispersive bands, which is neglected in the derivation of Eq. (6). Nevertheless, the small difference between  $\frac{\kappa_{\pm}(\tau)}{\tau}$  at  $\tau = 0.02$  and 0.1 indicates that such coupling is weak.

For  $N > 2$ , the construction of the first  $N - 2$  basis functions in the  $N$ -fold flat band subspace is straightforward: any dark states that do not overlap with  $x = 0$  are eigenfunctions of  $\mathbf{H}_1$ , as we have mentioned. For the remaining two doublet states, we use mathematical induction to find their approximate forms. Assuming that we have solved the  $(N - 2)$  case and found the correct doublet states  $\phi_1^{(N-2)}, \phi_2^{(N-2)}$ , we then approximate the correct doublet states in the  $N$  case by

$$\phi_1^{(N)} \approx \phi_1^{(N-2)} + cV(-N/2) + dV(N/2), \quad (7)$$

$$\phi_2^{(N)} \approx \phi_2^{(N-2)} + dV(-N/2) + cV(N/2), \quad (8)$$

where  $c, d$  are two real numbers. The basic assumption is that the central part of  $\phi_1^{(N)}, \phi_2^{(N)}$  near  $x = 0$  are insensitive to  $N$ , as we have seen in Figs. 3(a) and (b). It is easy to check that  $\langle \phi_1^{(N)} | \mathbf{H}_1 | \phi_2^{(N)} \rangle = 0$ , using  $\langle \phi_1^{(N-2)} | \mathbf{H}_1 | \phi_2^{(N-2)} \rangle = 0$ , and by requiring  $\langle \phi_1^{(N)} | \phi_2^{(N)} \rangle = 0$ , we find

$$cd(2J^2 + G^2) + 2J(c\delta^{(N-2)} + d\epsilon^{(N-2)}) = 0, \quad (9)$$

where  $\epsilon^{(N-2)}, \delta^{(N-2)}$  are the first (last) and last (first) elements of  $\phi_1^{(N-2)} (\phi_2^{(N-2)})$ . An additional constraint imposed by the degenerate perturbation theory is that there exists a superposition of  $V(-N/2), V(N/2)$  that is orthogonal to  $\phi_1^{(N)}, \phi_2^{(N)}$ . By defining it as  $\phi_3^{(N)} = V(-N/2) + eV(N/2)$ , we find

$$J\delta^{(N-2)} + e\epsilon^{(N-2)} + (ce + d)(2J^2 + G^2) = 0, \quad (10)$$

$$e\delta^{(N-2)} + J\epsilon^{(N-2)} + (c + ed)(2J^2 + G^2) = 0, \quad (11)$$

using  $\langle \phi_3^{(N)} | \phi_1^{(N)} \rangle = \langle \phi_3^{(N)} | \phi_2^{(N)} \rangle = 0$ . The solution of the above three nonlinear equations gives the value of  $c, d, e$ . Once  $c$  is found, we immediately know that the first four

elements of  $\phi_1^{(N)}$  are  $cJ, -cG, cJ + \epsilon^{(N-2)}, -\epsilon^{(N-2)}G/J$ . The localization length  $\xi$  can then be defined as

$$\xi^{-1} = \ln \left| \frac{\epsilon^{(N-2)}}{cJ} \right|, \quad (12)$$

using the values of the wave function on the first  $C$  site (i.e.,  $-cG$ ) and the second  $C$  site (i.e.,  $-\epsilon^{(N-2)}G/J$ ) from the left. For  $G = J = 1$ , we found that the solution  $c = -\epsilon^{(N-2)}/3$ ,  $d = -\delta^{(N-2)}/3$ ,  $e = -1$  accounts for the exponential tails shown in Fig. 3(c), and Eq. (12) gives  $\xi = \ln 3 \approx 1.10$ , which agrees reasonably well with the result of numerical fitting, i.e.,  $\xi = 1.03$ .

For the slope  $\kappa'_\pm(\tau)$  of the doublet states, a recursive relation can then be formulated. Assuming  $\phi_1^{(N)}$  is amplifying, we find

$$\begin{aligned} \kappa'_+{}^{(N)} &= \frac{\langle \phi_1^{(N)} | \mathbf{H}_1 | \phi_1^{(N)} \rangle}{\langle \phi_1^{(N)} | \phi_1^{(N)} \rangle} \\ &= \frac{3\kappa'_+{}^{(N-2)} - (\delta^{(N-2)2} - \epsilon^{(N-2)2})}{3 - (\delta^{(N-2)2} + \epsilon^{(N-2)2})}. \end{aligned} \quad (13)$$

It is clear that  $\kappa'_+{}^{(N)}$  (and similarly  $\kappa'_-{}^{(N)}$ ) becomes insensitive to  $N$  as  $N$  becomes large, because  $\epsilon^{(N-2)}, \delta^{(N-2)}$  are at the very ends of the exponentially decaying tails of  $\phi_1^{(N-2)}$ , leading to a converging series  $\kappa'_+{}^{(N)} \approx \kappa'_+{}^{(N-2)}$ . Using  $\kappa'_+{}^{(2)} = 0.707$  given by Eq. (6), we successively find  $\kappa'_+{}^{(4)} = 0.673$ ,  $\kappa'_+{}^{(6)} = 0.669$ ,  $\kappa'_+{}^{(8)} = 0.669$ , which agree well with the previously mentioned numerical values.

#### IV. EFFECT OF DISORDER

Unlike the doublet states, the  $\mathcal{PT}$ -broken dark states in the two degenerate manifolds can be randomly positioned along the lattice, but they are strictly confined either on the gain or loss half of the lattice. Due to their degeneracy, any arbitrary superpositions of them are still eigenstates of the system, and one can always find pairs of them such that they are  $\mathcal{PT}$ -symmetric partners of each other. However, the relevant superpositions are determined by the disorder in the system. Here we model the disorder by a white noise with a uniform distribution in  $[-W/2, W/2]$  around  $\omega_0$  on each lattice site. As the lower mode in Figs. 5(a-c) shows, if a flat band mode in the two degenerate manifolds is already confined to the loss (or gain) half of the lattice at small  $\tau$ , increasing  $\tau$  has little effect on its spatial profile. However, if at small  $\tau$  one of these modes occurs in both the gain and loss region, it will be forced to take either the gain half or the loss half, as the upper mode in Figs. 5(a-c) shows. Here the prevailing effect of  $i\tau\mathbf{H}_1$  is its non-Hermiticity, separating the lattice into a gain half and loss half.

In contrast, the prevailing effect of  $i\tau\mathbf{H}_1$  on the doublet states is its point defect mentioned previously. At very small  $\tau$ , the doublet states are localized by disorder,

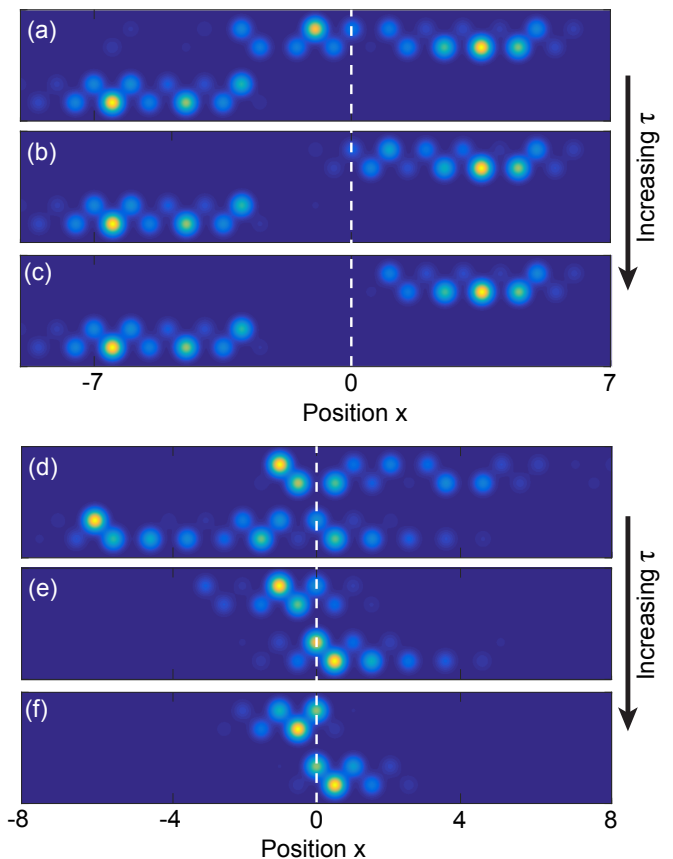


FIG. 5. (Color online) (a)-(c) Evolution of the dark states in the  $N/2 - 1$  degenerate flat band manifold from  $\tau = 5 \times 10^{-4}$ , 0.01, to 0.075. (d-f) The same for the doublet states. The color scale and legend are the same as in Figs. 3(a) and (b). The amplitude of onsite white noise is  $W = 0.05$  and  $N = 20$ .

i.e., they are Anderson localized [41], and the localization length can be rather long in a particular disorder realization (although on average the localization length is not much longer than that determined by the point defect [19]). As  $\tau$  increases, the point defect in  $\mathbf{H}_1$  gradually prevails over the white noise disorder, and the doublet states approach their spatial patterns in the absence of  $W$ , as can be seen from Figs. 5(e-f) in comparison with Fig. 3. In other words, the  $\mathcal{PT}$ -symmetric relation  $\phi_1 = \mathcal{PT}\phi_2$  of the doublet states is restored as  $\tau$  increases. The same cannot be said about the other flat band modes in general, due to the presence of disorder that breaks the  $\mathcal{PT}$  symmetry.

Finally, we find that disorder has a stronger effect on the dispersive bands than the flat band in terms of  $\mathcal{PT}$  breaking, probably because the flat band modes can avoid the disorder on  $B$  sites, where they are black. As Fig. 6 shows, the disorder smoothes out the  $\mathcal{PT}$ -transitions of the dispersive band modes in Fig. 4, but the thresholdless  $\mathcal{PT}$  breaking of the flat band modes is largely unaffected. Upon careful inspection, we find that one flat band mode with  $\kappa_- \approx -\tau$  deviates slightly from the other 2 in this

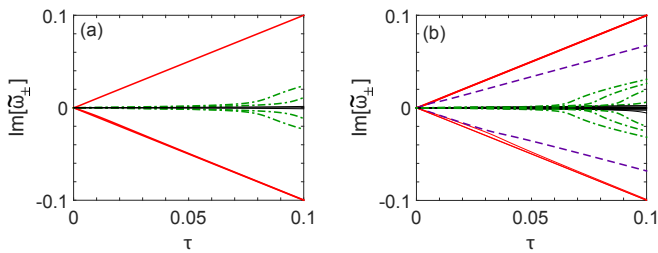


FIG. 6. (Color online) Same as Fig. 4 but with disorder. The amplitude of onsite white noise is  $W = 0.05$ .

branch at small  $\tau$  but rejoins the latter as  $\tau$  increases. This behavior is due to its spatial profile change, similar to that of the upper mode in Figs. 5(a-c), but here this mode is forced to take the loss side: when this mode has a small portion in the gain half of the lattice at small  $\tau$ , overall it feels less loss and hence its negative  $\kappa_-$  is larger than  $-\tau$ . As its spatial profile is squeezed into the loss half of the lattice by the growing  $\mathcal{T}$ -breaking perturbation, it feels more loss than before and its  $\kappa_-$  approaches its minimum value  $-\tau$ . We can also infer that the other 2 modes in this branch are localized already in the loss half when  $\tau$  is small, which is verified by inspecting their spatial profiles (not shown).

## V. CONCLUSION

In summary, we have shown that by introducing a  $\mathcal{PT}$ -symmetric perturbation to a quasi-1D Lieb lattice, two different scenarios of thresholdless  $\mathcal{PT}$  symmetry breaking can take place in the flat band, depending on whether the degeneracy  $N$  in the flat band is even or odd. The two degenerate manifolds with  $\kappa_{\pm} = \pm\tau$  always exist and undergo thresholdless  $\mathcal{PT}$  breaking. While their center positions are random, they are confined to either the gain half or the loss half of the lattice in the absence of disorder. This feature holds even with disorder, when the  $\mathcal{PT}$ -symmetric perturbation is strong enough. In contrast, the  $\mathcal{PT}$ -symmetric doublet states only exist when  $N$  is even, and they display weaker non-Hermiticity than the degenerate manifolds. These doublet states are pinned at the symmetry plane with exponential tails in the gain and the loss halves. These tails are the result of a point defect in the  $\mathcal{PT}$ -symmetric perturbation at  $x = 0$ , instead of its half-gain-half-loss nature as previously found [40]. The disorder may disturb their spatial profiles at weak  $\mathcal{T}$ -breaking perturbation, but as the latter increases, this feature is restored, together with the  $\mathcal{PT}$ -symmetry relation between the two doublet states.

We thank Hakan Türeci, Bo Zhen, and Vadim Oganessian for helpful discussions. This project is supported by NSF under Grant No. DMR-1506987.

- 
- [1] V. Apaja, M. Hyrkäs, and M. Manninen, Phys. Rev. A **82**, 041402(R) (2010).
- [2] M. Hyrkäs, V. Apaja, and M. Manninen, Phys. Rev. A **87**, 023614 (2013).
- [3] M. C. Rechtsman, J. M. Zeuner, A. Tünnermann, S. Nolte, M. Segev, and A. Szameit, Nature Photonics **7**, 153 (2013).
- [4] R. A. Vicencio, C. Cantillano, L. Morales-Inostroza, B. Real, C. Mejía-Cortés, S. Weimann, A. Szameit, and M. I. Molina, Phys. Rev. Lett. **114**, 245503 (2015).
- [5] S. Mukherjee, A. Spracklen, D. Choudhury, N. Goldman, P. Öhberg, E. Andersson, and R. R. Thomson, Phys. Rev. Lett. **114**, 245504 (2015).
- [6] C. L. Kane and E. J. Mele, Phys. Rev. Lett. **78**, 1932 (1997).
- [7] F. Guinea, M. I. Katsnelson, and A. K. Geim, Nature Phys. **6**, 30 (2010).
- [8] A. Simon, Angew. Chem. **109**, 1873 (1997).
- [9] S. Deng, A. Simon, and J. Köhler, Angew. Chem. **110**, 664 (1998).
- [10] S. Deng, A. Simon, and J. Köhler, J. Solid State Chem. **176**, 412 (2003).
- [11] M. Imada and M. Kohno, Phys. Rev. Lett. **84**, 143(2000).
- [12] E. Tang, J-W. Mei, and X-G. Wen, Phys. Rev. Lett. **106**, 236802 (2011).
- [13] T. Neupert, L. Santos, C. Chamon, and C. Mudry, Phys. Rev. Lett. **106**, 236804 (2011).
- [14] S. Yang, Z.-C. Gu, K. Sun, and S. Das Sarma, Phys. Rev. B **86**, 241112(R) (2012).
- [15] T. Jacqmin, I. Carusotto, I. Sagnes, M. Abbarchi, D. D. Solnyshkov, G. Malpuech, E. Galopin, A. Lemaître, J. Bloch, and A. Amo, Phys. Rev. Lett. **112**, 116402 (2014).
- [16] F. Baboux, L. Ge, T. Jacqmin, M. Biondi, A. Lematre, L. Le Gratiet, I. Sagnes, S. Schmidt, H. E. Türeci, A. Amo, and J. Bloch, arXiv:1505.05652.
- [17] D. Leykam, S. Flach, O. Bahat-Treidel, and A. S. Desyatnikov, Phys. Rev. B **88**, 224203 (2013).
- [18] S. Flach, D. Leykam, J. D. Bodyfelt, P. Matthies, and A. S. Desyatnikov, Europhys. Lett. **105**, 30001 (2014).
- [19] L. Ge and H. E. Türeci, in preparation.
- [20] C. M. Bender and S. Boettcher, Phys. Rev. Lett. **80**, 5243 (1998).
- [21] C. M. Bender, S. Boettcher, and P. N. Meisinger, J. Math. Phys. **40**, 2201 (1999).
- [22] C. M. Bender, D. C. Brody, and H. F. Jones, Phys. Rev. Lett. **89**, 270401 (2002).
- [23] R. El-Ganainy, K. G. Makris, D. N. Christodoulides, and Z. H. Musslimani, Opt. Lett. **32**, 2632 (2007).
- [24] S. Klaiman, U. Gunther, and N. Moiseyev, Phys. Rev. Lett. **101**, 080402 (2008).
- [25] Z. H. Musslimani, K. G. Makris, R. El-Ganainy, D. N. Christodoulides, Phys. Rev. Lett. **100**, 030402 (2008).
- [26] K. G. Makris, R. El-Ganainy, D. N. Christodoulides, and Z. H. Musslimani, Phys. Rev. Lett. **100**, 103904 (2008).
- [27] T. Kottos, Nat. Phys. **6**, 166 (2010).
- [28] S. Longhi, Phys. Rev. A **82**, 031801(R) (2010).
- [29] Y. D. Chong, L. Ge, and A. D. Stone, Phys. Rev. Lett. **106**, 093902 (2011).
- [30] L. Ge, Y. D. Chong, and A. D. Stone, Phys. Rev. A **85**,

- 023802 (2012).
- [31] P. Ambichl, K. G. Makris, L. Ge, Y. D. Chong, A. D. Stone, and S. Rotter, *Phys. Rev. X* **3**, 041030 (2013).
- [32] Z. Lin, J. Schindler, F. M. Ellis, and T. Kottos, *Phys. Rev. A* **85**, 050101(R) (2012).
- [33] S. Bittner *et al.* *Phys. Rev. Lett.* **108**, 024101 (2012).
- [34] A. Regensburger *et al.* *Nature (London)* **488**, 167 (2012).
- [35] N. Bender *et al.* *Phys. Rev. Lett.* **110**, 234101 (2013).
- [36] B. Peng *et al.* *Nature Phys* **10**, 394-398 (2014).
- [37] L. Feng, Z. J. Wong, R. Ma, Y. Wang, and X. Zhang, *Science* **346**, 972-975 (2014).
- [38] H. Hodaei, M.-A. Miri, M. Heinrich, D. N. Christodoulides, and M. Khajavikhan, *Science* **346**, 975-978 (2014).
- [39] L. Ge and A. D. Stone, *Phys. Rev. X* **4**, 031011 (2014).
- [40] L. Ge, Y. D. Chong, S. Rotter, H. E. Türeci, and A. D. Stone, *Phys. Rev. A* **84**, 023820 (2011).
- [41] P. W. Anderson, *Phys. Rev.* **109**, 1492-1505 (1958).
- [42] B. Zhen, C. W. Hsu, Y. Igarashi, L. Lu, I. Kaminer, A. Pick, S.-L. Chua, J. D. Joannopoulos, M. Soljai arXiv:1504.00734.
- [43] R. Shanker, *Principles of Quantum Mechanics*, 2nd ed. (Springer, New York, 1994).